05

High-NA focusing of ultrashort laser pulses in bulk of ZnSe

© Yu.S. Gulina[1,2], S.I. Kudryashov[2], N.A. Smirnov[2], E.V. Kuzmin[2]

[1] Bauman Moscow State Technical University, Moscow, Russia
[2] Lebedev Physical Institute, Russian Academy of Sciences, Moscow, Russia

e-mail: julia-sg@yandex.ru

Received on December 20, 2021
Revised on December 20, 2021
Accepted on December 30, 2021

A study of high-NA focusing process of ultrashort laser pulses in bulk of ZnSe has been carried out. It is shown that when focusing laser Gaussian beam with high-aperture lenses into a transparent medium aberration distortions occur leading to an increase in focal spot size. The results of experimental studies on ablation of front and back surfaces of a plane-parallel plate with 4 mm thickness made of ZnSe by laser pulses with a duration of 0.3 ps, 1 ps, 10 ps and a wavelength of 1030 nm focused by a micro lens ($NA = 0.55$) are presented. It is shown that at low pulse energies focusing can be considered in a linear mode in which focal spot size is due to aberration distortions.

Keywords: direct laser writing, femtosecond laser pulses, high-NA focusing, ablation, aberrations.

DOI: 10.21883/EOS.2022.04.53724.45-21

Introduction

At the present time, the possibilities of using laser processing methods with the help of ultrashort pulses for the manufacture of complex structures and devices are being actively studied [1–4]. Direct laser writing can be used to create complex 3D spatial structures with submicron resolution inside transparent media. Such structures are needed for the development of information & telecommunication and bioengineering applications of the next generation: optical memory [5], micro-optical components [6], refractive-index gratings [7], optical waveguides [8] etc.. High precision, processing speed and versatility make ultrashort pulse laser processing an important tool for manufacturing. To ensure maximum processing efficiency, high-NA focusing of laser radiation in bulk of a modified transparent medium is used, which makes it possible to obtain the necessary above-threshold value of the laser radiation intensity and local energy deposition in the focusing region [9].

The laser energy is mainly absorbed in the focal spot due to the nonlinear features of the interaction of the laser with the dielectric [10,11]. Energy absorption leads to material modification, and the size of the ablation regions seems to be one of the most important parameters that affect the efficiency as well as the spatial resolution of microscopic treatment. For threshold modification processes such as ablation, the radius of the modified region depends on the threshold fluence F_{th}, the pulse energy E, and the focal laser spot radius w_0 determined by [12] by energy level $1/e$:

$$R_{abl}^2(w_0^2) = w_0^2 \ln\left(\frac{E}{F_{th}\pi w_0^2}\right). \qquad (1)$$

Most commonly, the physical effects used to create controlled damage within materials being treated, require focusing the laser beam into a small spot, typically a few micrometers in size. This is achieved through the use of high-aperture object lenses or specially designed aspherical lenses that are corrected for the specific working plane in air or within the transparent medium such as the back of the coverslip. Therefore, the size of the spot in a predetermined working plane is determined by the wave nature of light, i.e. is diffraction-limited.

When focusing a Gaussian beam in air, its radius at given distance z from the object lens can be determined as

$$w(z) = w_0\sqrt{1 + \left(\frac{z - f'}{z_R}\right)^2}, \qquad (2)$$

where $z = f'$ is the distance to the geometric focus, and $z_R = \frac{\pi w_0^2}{\lambda}$ is Rayleigh length, λ is laser wavelength, $w_0 = \frac{\lambda f'}{\pi w(0)}$ is focal spot radius, which can also be expressed in terms of the numerical aperture NA of the focusing optics:

$$w_0 = \frac{\lambda}{\pi}\frac{\sqrt{1 - NA^2}}{NA},$$

$w(0)$ is laser beam radius in front of the focusing system.

When Gaussian beam is focused into a transparent material in the paraxial approximation, the displacement in position of the focal plane occurs. In this case, the size of the focused spot is similar to the size of the spot in air, and the Rayleigh distance increases in proportion to the refractive index of the material:

$$z_{R(mat)} = n\frac{\pi w_0^2}{\lambda} = n z_{R(air)}.$$

In practice, when the Gaussian beam is focused at different depths within transparent medium, positive spherical aberration occurs, affecting the size of the focused spot. For numerical apertures $NA > 0.5$, the size of the focal spot can be several times larger than the diffraction-limited spot [13].

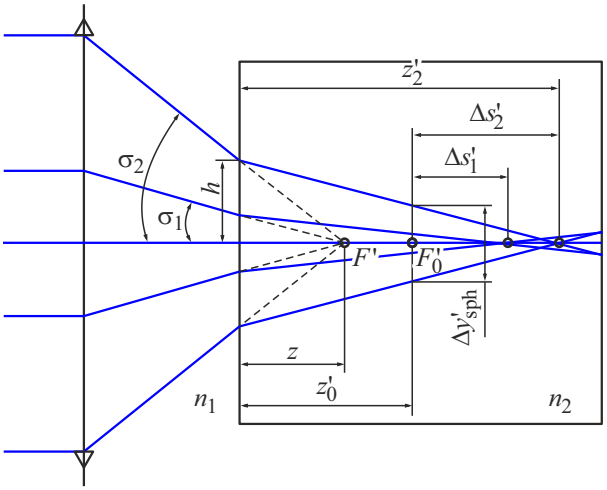

Figure 1. Calculation scheme for determining the spherical aberration.

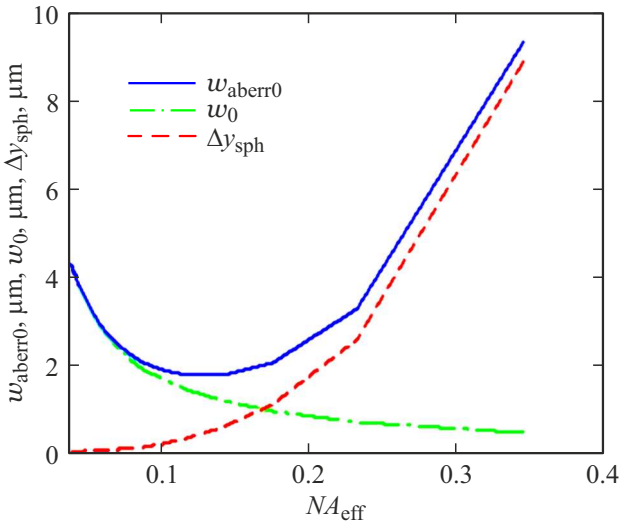

Figure 2. Dependence of the paraxial and aberrational spot sizes, as well as spherical aberration on the effective numerical aperture.

This inevitably affects the concentration of laser energy in the focused spot and reduces the spatial resolution of the laser modification. To minimize the influence of aberrations on the focal spot size optics with lower apertures can be used; however, in the case of significant pulse energies, focusing will be distorted by nonlinear effects: Kerr self-focusing, plasma formation, filamentation.

The positive spherical aberration that occurs when the focused beam passes through the air-material interface causes the displacement in position of the focusing plane relative to the paraxial position, and for different beam zones this displacement will be different i.e. from the maximal one for the edge zone to the minimal one for the central zone (Fig. 1).

The value of the maximum longitudinal displacement of focusing plane $\Delta s_2'$ can be estimated from the formula

$$\Delta s_2' = z_2' - z_0' = \frac{n_2}{n_1}\sqrt{h^2\left(1 - \frac{n_1^2}{n_2^2}\right) + \frac{z_0'^2}{n_2}} - z_0', \qquad (3)$$

where z_2' is the distance from the interface to the plane of focusing of the extreme rays of the beam, z_0' is the distance from the interface to the paraxial focal plane, n_1 and n_2 are refractive indices of the media, h is radius of the focused beam at the media interface.

In the paraxial focal plane, the longitudinal displacement of the focusing planes (3) leads to the appearance the transverse spherical aberration $\Delta y_{sph}'$, the value of which can be determined by the formula

$$\Delta y_{sph}' = \Delta s_2' \operatorname{tg}\left(\frac{h}{z_2'}\right). \qquad (4)$$

The larger the numerical aperture of the focusing optics, or the deeper the beam is focused inside the transparent medium, the greater the spherical aberration and, consequently, the greater the scattering of light energy in the

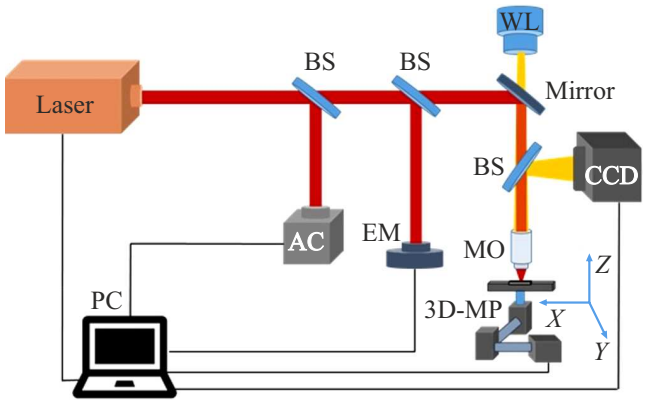

Figure 3. Schematic of fs/ps-laser ablation workstation: BS — beam splitter, EM — energy meter, AC — autocorrelator, MO — microscope objective lens, WL — white-light illumination source, PC — computer with dedicated control software laser, camera, positioning system, CCD — camera for surface visualization during scanning.

focal region. The size of the focal spot, taking into account aberrational distortions (4), will be determined as

$$w_{aberr0} = w_0 + \Delta y_{sph}'. \qquad (5)$$

Thus, increasing the aperture, on the one hand, leads to decrease in the paraxial spot, and on the other hand, to aberrational increase, because of this it is necessary to determine the optimal numerical aperture that ensures the minimum size of the focused spot or use adaptive correction for spherical aberration. Fig. 2 shows the dependences of the paraxial and aberrational spot sizes, as well as spherical aberration on the effective numerical aperture. The effective numerical aperture is determined through the size of the

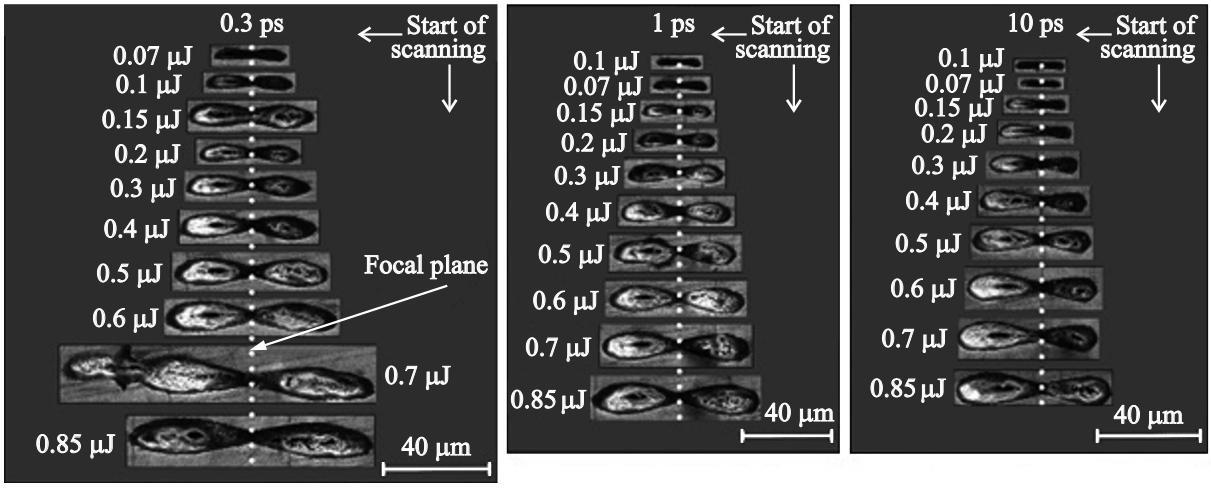

Figure 4. Ablation regions on the front surface of the sample.

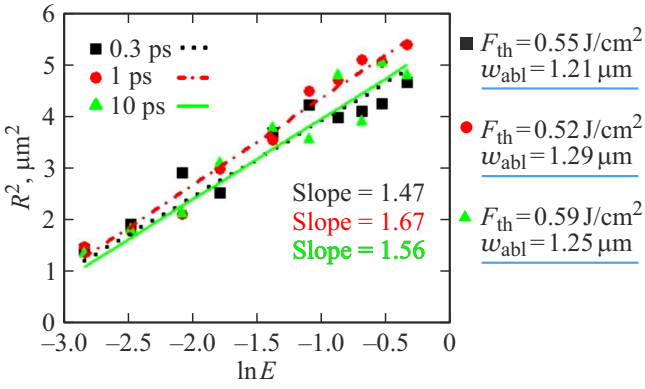

Figure 5. Dependence of the squared radius of the ablation region on the front sample surface on the pulse energy logarithm.

focused spot on the interface as well as the focusing depth:

$$NA_{eff} = \sin\left(\text{arctg}\left(\frac{h}{z_0'}\right)\right).$$

Thus, the size of the ablation region at a given distance z from the object lens, taking into account formulas (1), (2) and (5), can be determined by the proposed formula

$$R^2_{abl_{aberr}}(z) = w^2_{aberr}(z)\ln\left(\frac{E}{F_{th}\pi w^2_{aberr}(z)}\right), \qquad (6)$$

where the size of the focused beam at a given distance z is determined taking into account aberrational distortions:

$$w_{aberr}(z) = w_{aberr0}\sqrt{1+\left(\frac{z-f'}{z_{R(mat)}}\right)^2}.$$

Experimental part

To evaluate the effect of aberrational distortions on the high-NA focusing of a Gaussian beam in bulk of transparent

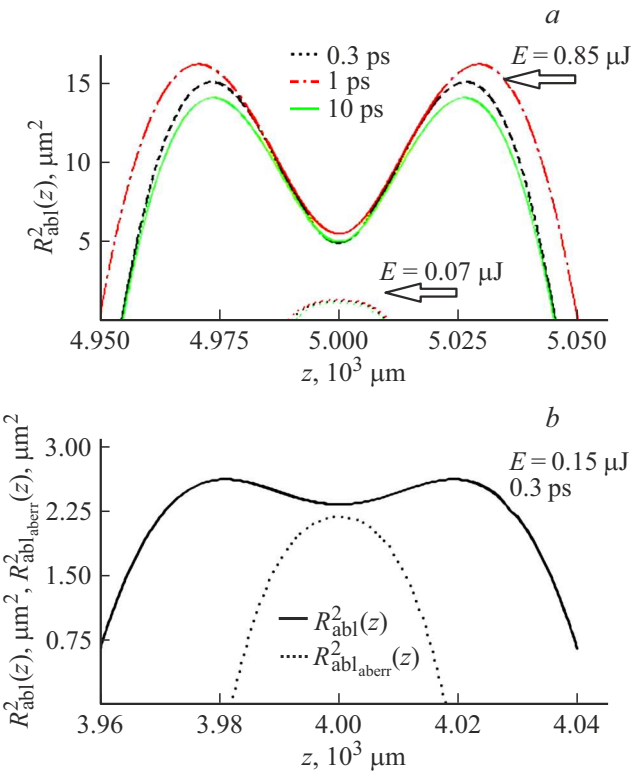

Figure 6. Dependences of the squared radius of the ablation region on the front surface on the distance from the objective lens (a) and the squared radius of the ablation region on the back surface on the distance from the interface (b).

dielectrics, a number of experimental studies were carried out, during which the front and rear sides of the sample in the form of the plane-parallel plate with thickness of 4 mm, polished on both sides, made of ZnSe material,were ablated. The schematic of experimental setup used for laser ablation is shown in Fig. 3.

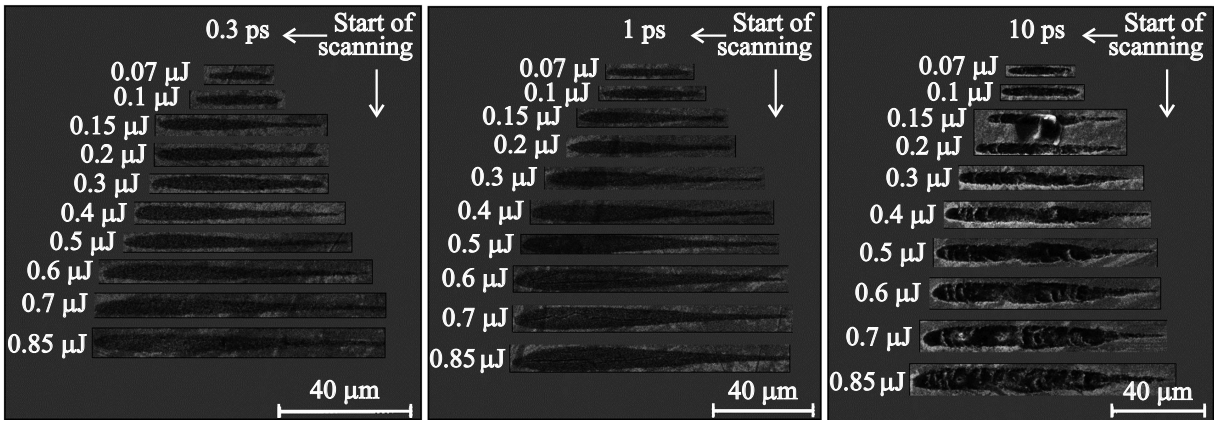

Figure 7. Ablation regions on the rear surface of the sample.

Fiber Yb^{+3} ion laser by Satsuma (Amplitude Systemes) with wavelength of 1030 nm and linear polarization, as source of laser radiation was used. The pulse durations, controlled by the built-in compressor, was 0.3, 1, and 10 ps, and the pulse repetition rate was 0.2 kHz. The sample was fasten on the three-coordinate movable platform, which made it possible to perform two-coordinate scanning $Z-Y$ — the changing the focusing depth together with the movement of the sample, which ensured consistent focusing (within the volume of the sample — on surface of the sample – above the sample surface). In this case, when the rear side was irradiated, radiation was applied directly through the front side of the sample. For focusing, the microscope objective lens with $NA = 0.55$ and focal length $f = 5$ mm was used. Ablation craters were obtained at pulse energies from 0.07 to 0.85 μJ and dynamic focusing of the laser beam. The laser radiation energy was measured using an Ophir PD10-C energy meter.

Results and discussion

Front surface ablation was performed to calibrate and determine material modification thresholds. Images of the experimental ablation regions obtained with a Tescan Vega Compact scanning electron microscope (SEM) are shown in Fig. 4.

Based on measurements of the transverse dimensions of these regions, dependences of the squared radius of the ablation crater R^2_{abl} on the energy logarithm $\ln E$ were plotted for different pulse durations (Fig. 5). The slope of the obtained dependences [14] determines the characteristic sizes of the focal spots $w_{abl} = (\text{Slope})^{1/2}$, which are close to the theoretically calculated values of the focal spot $w_0 = 1.2\,\mu$m for laser beam with radius by level of $1/e$ $w(0) = 0.7$ mm. The values of the modification thresholds calculated in terms of the threshold energies for various pulse durations $F_{th} = E_{th}/(\pi w^2_{abl})$ are shown in Fig. 5.

Theoretically determined on the basis of the proposed formula (6), the shapes of the ablation regions are in good agreement with the type of experimentally obtained burns on the front surface of the sample (Fig. 6, *a*): for low pulse energies, the shape of the burns is smooth, and for high ones, a characteristic bend is observed in the region of the focusing plane i.e.burns are dumbbell-shaped.

The images of ablation regions on the rear surface of the sample obtained with the Tescan Vega Compact SEM are shown in Fig. 7.

Dependences of the squared width of the ablation crater R^2_{abl} on the logarithm of the energy $\ln E$ for different pulse durations, obtained by measuring the ablation regions on the rear surface of the sample, as well as the characteristic sizes of focal spots and the values of modification thresholds, are shown in Fig. 8. In the region of low pulse energies, the characteristic sizes obtained from the dependences $R^2_{abl} - \ln E$ agree with the theoretically calculated size of the focal spot allowing for aberration blurring effect $w_{aberr} = 1.8\,\mu$m.

The shape of the dependences of the squared ablation radius on distance, calculated on the basis of formula (6), which takes into account the aberration, for the low-energy region also agrees with the type of experimental burns; they have an oval shape. While without taking into account aberrational distortions, the theoretical form is dumbbell shaped (Fig. 6, *b*). However, in the region of high pulse energies, the mismatch between the theoretical and experimentally obtained characteristic sizes of focal spots is showed, even when aberrational distortions are taken into account, i.e. the theoretically calculated values are underestimated relative to the experimental ones. Apparently this is related with a non-linear nature of focusing, due to the presence of Screening bulk plasma, self-focusing and filamentation that arise at high energies. It should be noted that the presence of nonlinear effects during strong focusing into the volume of transparent materials is due to a decrease in the effective focusing aperture at the air-medium interface in proportion to the refractive index of the medium. Thus, even when

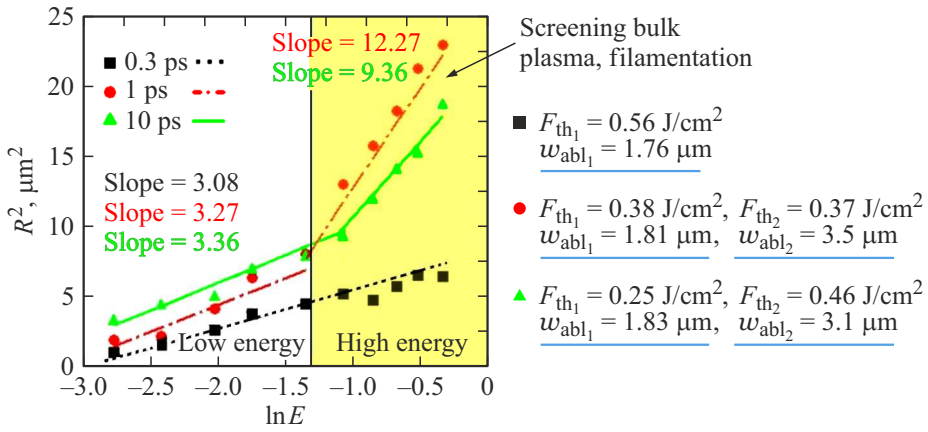

Figure 8. Dependence of the squared radius of the ablation region on the rear sample surface on the pulse energy logarithm.

using objective lenses with high apertures to focus in bulk of transparent media with high refractive index, the effective working aperture is reduced, so there is no attenuation of non-linear effects.

Conclusion

The process of high-NA focusing of ultrashort laser pulses in bulk of ZnSe has been studied. It is shown that when analyzing the size of the focal spot, it is necessary to take into account the spherical aberration arising from the distortion of the wave front of focused Gaussian beam at the air-material interface. It is noted that in the range of low pulse energies, there is a good agreement between the values of the characteristic ablation radii calculated taking into account aberrational distortions and the experimentally obtained values, which indicates a linear nature of focusing, in which the size of the focal spot is defined to the presence of spherical aberration. In the region of high pulse energies, with high-NA focusing of ultrashort laser pulses bulk of ZnSe, as well as other transparent materials with a high refractive index, focusing proceeds in a nonlinear mode due to decrease in the effective working aperture.

Funding

The authors are grateful to the Russian Science Foundation for the financial support of these studies within the framework of project 21-79-30063.

Conflict of interest

The authors declare that they have no conflict of interest.

References

[1] L. Cerami, E. Mazur, S. Nolte, C. B. Schaffer. *Ultrafast nonlinear optics* (Springer, Heidelberg, 2013), p. 287–321. DOI: 10.1007/978-3-319-00017-6_12

[2] K.C. Phillips, H.H. Gandhi, E. Mazur, S.K. Sundaram. Advances in Optics and Photonics, **7** (4), 684 (2015). DOI: 10.1364/AOP.7.000684

[3] R. R. Gattass, E. Mazur. Nature Photonics, **2** (4), 219 (2008). DOI: 10.1038/nphoton.2008.47

[4] K. Sugioka, Y. Cheng. Light Sci Appl., **3**, e149 (2014). DOI: 10.1038/lsa.2014.30

[5] M.H. Hong et al. Appl. Phys. A, **79**, 791 (2004). DOI: 10.1007/s00339-004-2630-1

[6] J. Qiu, K. Miura, K. Hirao. Optical Components and Materials, **5350**, 1 (2004). DOI: 10.1117/12.537372

[7] Y. Shimotsuma, P.G. Kazansky, J. Qiu, K. Hirao. Phys. Rev. Lett., **91**, 247405 (2003). DOI: 10.1103/PhysRevLett.91.247405

[8] F. Chen, J.V. de Aldana. Laser Photonics Rev., **8** (2), 251 (2014). DOI: 10.1002/lpor.201300025

[9] C.B. Schaffer, A. Brodeur, J.F. Garcia, E. Mazur. Optics Lett., **26** (2), 93 (2001). DOI: 10.1364/OL.26.000093

[10] J. Peng, D. Grojo, D.M. Rayner, P.B. Corkum. Appl. Phys. Lett., **102**, 161105 (2013). DOI: 10.1063/1.4802820

[11] R.R. Gattass, E. Mazur. Nat. Photonics, **2**, 219 (2008). DOI: 10.1038/nphoton.2008.47

[12] S. Kudryashov, P. Danilov, A. Rupasov, S. Khonina, A. Nalimov, A. Ionin, G. Krasin, M. Kovalev. Optical Materials Express, **10** (12), 3291 (2020). DOI: 10.1364/OME.412399

[13] A. Laskin, V. Laskin, A. Ostrun. ICALEO, **2017**, M404 (2017). DOI: 10.2351/1.5138167

[14] J.M. Liu. Optics Lett., **7** (5), 196 (1982). DOI: 10.1364/OL.7.000196